WATER RESOURCES RESEARCH, VOL. 22, NO. 6, PAGES 869–875, JUNE 1986

# Differential Bare Field Drainage Properties From Airborne Microwave Observations

R. BERNARD, J. V. SOARES, AND D. VIDAL-MADJAR

*Centre National d'Etudes des Télécommunications, Centre National de la Recherche Scientifique/Centre de Recherche sur la Physique de l'Environment, Issy-les-Moulineaux, France*

Time variations of the surface soil moisture can be monitored using active microwave remote sensing. With the existence of airborne systems, it is now possible to estimate this variable on a regional scale. Data from a helicopter-borne scatterometer show that the surface water content reductions during a 9-day period are quite different from one field to another. A simple model describing the water budget of the soil surface layer due to evaporation and drainage is applied. From this model, a pseudodiffusivity can be calculated for each field using only the remotely sensed data. This new parameter gives a quantitative estimate of the observed drying heterogeneities.

## 1. INTRODUCTION

It is now common to characterize a soil by its physical hydraulic properties, in particular, as functions of water pressure head $h$ and hydraulic conductivity $K$. These functions can be obtained in the laboratory or, with some difficulties, in the field. The usefulness of this characterization for vertical water movement simulation in the soil is widely accepted [*Philip*, 1975]. Its methodological drawback is that it is only applicable to local studies. This is due to the important spatial variability of the $h$ and $K$ functions, which prevents the extension of a one-point measurement to the entire field [*Nielsen et al.*, 1973; *Vauclin et al.*, 1983]. For many reasons (water shed and atmospheric models, irrigation, drainage, etc.), even a rough mapping of the hydraulic behavior of the soil layer directly in contact with the atmosphere (precipitation and evaporation) may be useful. This goal is not reasonably accessible to in situ investigations. Other means must be found. Among possible candidates is active microwave remote sensing. The capability of this technique to give an estimate of the soil surface mean moisture has been fully demonstrated experimentally [*Ulaby and Batlivala*, 1976; *Bradley and Ulaby*, 1981; *Jackson et al.*, 1981; *Bernard et al.*, 1982] as well as theoretically [*Ulaby et al.*, 1983; *Mo et al.*, 1984].

With the development of airborne systems, it is now possible to map regional water content and its variations on short and long time scales over bare or vegetated soils. Recently it has been shown that the variation in time of bare soil surface moisture is correctly described by the Richards equation [*Bernard et al.*, 1981]. But to solve the inverse problem (estimate a water budget from remote sensing data), it is necessary to know with good precision the hydraulic characteristics of the soil studied [*Prévot et al.*, 1984]. For this reason, the Richards equation is not applicable to large-scale mapping in the present state of the art. Nevertheless, these works have shown the physical relation that exists between the radar signal and vertical water movement in the first meter of the soil. Therefore it may be possible to find a simple model applicable to mapping that describes in a realistic way the mean exchanges between a surface layer and the atmosphere (evaporation) and the underlying soil (drainage). Such a model must be as physical as possible but be able to account for a certain amount of spatial heterogeneities in the soil properties. Built from an airborne experiment using the ERASME (etude radar des sols et de la mer) scatterometer [*Bernard and Vidal-Madjar*, 1983], the methodology proposed in this paper allows comparison of neighboring fields in terms of water diffusion from a surface layer.

In the first part of this presentation, the site and the experiment are described. In the next section, it is shown using ground data how ERASME measures the soil surface mean water content and what differences are observed between fields. The third part gives a description of the water budget model and its application to the experiment.



Paper number 5W4116.
0043-1397/86/005W-4116$05.00

## 2. DESCRIPTION OF THE EXPERIMENT

### 2.1. *Test Site and Ground Measurements*

Data used here are from an experiment held in a flat agricultural area (La Beauce) southwest of Paris. This area is characterized by large fields of wheat and corn. The surveyed region is a $6 \times 6$ km$^2$ area. In June, July, and September 1983 the helicopter-borne scatterometer was flown around noon local time almost every day. The aim was to map the surface soil moisture in order to study its spatial properties and time evolution under various conditions of climate, wetness, and vegetation canopies.

The data discussed here were obtained between September 20 and 29, 1983, which corresponds to a period of clear days without rain. The last rainfall occurred on September 19 (3.5 mm). The field area is presented in Figure 1. It consists mainly of bare soil, previously wheat covered, with some corn fields. On field 3, measurements of water content profiles were implemented to a depth of 65 cm until September 16 using neutron probe and tensiometer instruments. Net radiation, air temperature, and wind speed at 2 m were also available. Table 1 gives for each day the daily net radiation expressed in millimeters of water, the air temperature, and the wind speed at noon local time. The net radiation did not vary much, and the wind speed was low for the whole period.

The composition of soil samples from 0- to 10-cm depth of fields 3 and 4 was analyzed. Composition is uniformly 14% sand and 8.5% clay, corresponding to a silt loam. If the *Schmugge* [1980] formula is used, the soil field capacity equals 0.235 g/g. The soil density is 1.38 g/cm$^3$.

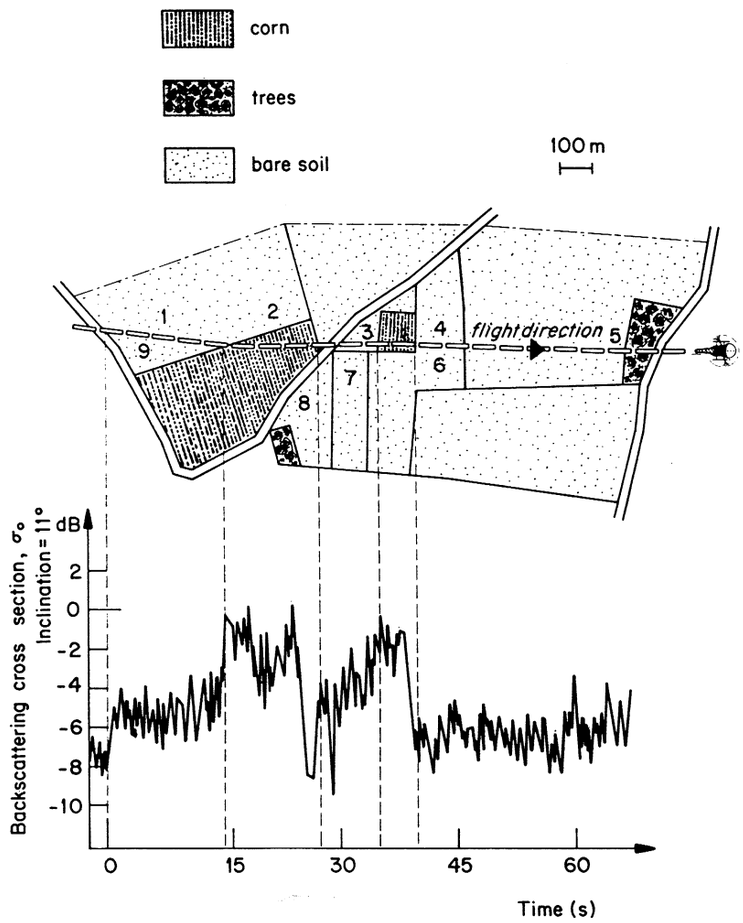


Fig. 1. An example of the ERASME flights and data. The map represents the test site. The considered fields are labeled 1–9. The corresponding radar signal is plotted. The roads are clearly visible. The signal from the corn fields is more intense than the bare soil response. On this curve, the spatial heterogeneities of the radar signal can be appreciated.

### 2.2. *The Scatterometer ERASME*

The scatterometer ERASME is an airborne frequency-modulated continuous wave radar that can be used on board a small helicopter. Its configuration was that considered optimal for a soil moisture mission (5.3 GHz, horizontal polarization, and 11° incidence angle). This instrument is fully described elsewhere [*Bernard and Vidal-Madjar*, 1983].

The area observed on the ground by the instrument is about 40 m$^2$. The signal is integrated for 200 ms, which is equivalent to a point every 6 m at a speed of 30 m/s. On the bottom of Figure 1 is plotted an example of the radar response over the test fields. The fluctuation of the signal is due to variations of soil surface properties such as water content and not to the fading, which was eliminated by using the time integration method.

A Barnes PRT 5 infrared radiometer is mounted together with the scatterometer. It gives the blackbody equivalent temperature of the observed surface simultaneously with the radar signal.

TABLE 1. Meteorological Data Measured on Field 3

| | September | | | | | | | | | |
|---|---|---|---|---|---|---|---|---|---|---|
| | 20 | 21 | 22 | 23 | 24 | 25 | 26 | 27 | 28 | 29 |
| $R_n$ (daily), mm of water | 3.2 | 1.46 | 2.42 | 2.97 | | 2.5 | 2.87 | 2.43 | 2.45 | |
| $T_a$,°C (2 m; 1200 LT) | 12 | 15 | 15 | 19 | 24 | 19 | 19 | 22 | 25 | 24 |
| $v_a$, m/s (2 m; 1200 LT) | 2.7 | 4.5 | 1.5 | 4.3 | 0.8 | 3.0 | 1.3 | 4.4 | 0.7 | 2.6 |

## 3. RESULTS

### 3.1. *Scatterometer Calibration for Soil Moisture*

Soil samples from 0- to 10-cm depth have been taken in fields 2, 3, 4, 7, and 8 and in the corn field between parcels 3 and 4 (Figure 1). For the entire campaign, 29 comparison points have been obtained after exclusion of the cases where the helicopter did not fly over the ground plots. The relationship between the radar backscattering for an inclination angle of 11° ± 1° and the measured soil water content was calculated from these data and is given in Figure 2. When $w$, water content in the first 10 cm, is expressed in cm$^3$/cm$^3$, the regression gives

$$w = 0.30 + 0.016\sigma_0 \; dB \qquad (1)$$

where $\sigma_0$ is the absolute backscattering coefficient average on the entire area of the fields.

The backscattering coefficient $\sigma_0$ is obtained with an error

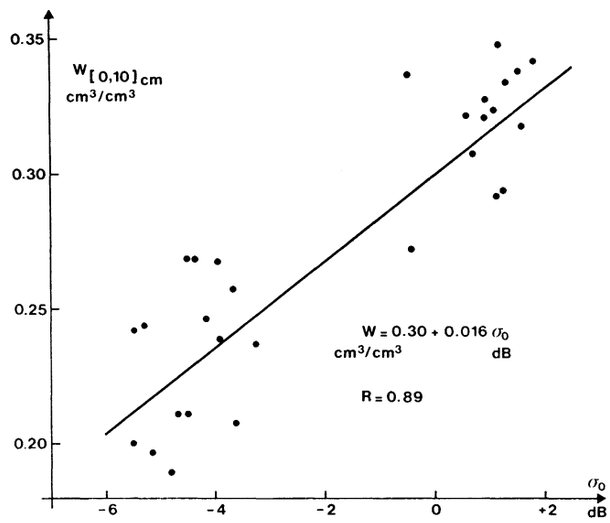


Fig. 2. Volumetric water content in the integrated 0- to 10-cm layer expressed in $cm^3/cm^3$ as function of the backscatter coefficient $\sigma_0$. The regression line is the algorithm used here to obtain the surface soil water from the radar data.

of about 0.5 dB [*Bernard and Vidal-Madjar*, 1983]. The standard deviation due to variation of the surface properties inside one field is roughly 1 dB.

The correlation coefficient equals 0.89, and the residual variance of $w$ is 0.018 $cm^3/cm^3$, lower than the variance of the ground measurements. This shows the linear relation between $\sigma_0$ and $w$ is meaningful. This value (0.018 $cm^3/cm^3$) is considered as the mean error made on the evaluation of the absolute surface soil moisture by using the radar response and the regression line.

### 3.2. *Spatial and Temporal Variations of Soil Moisture*

The variations of $w$ and $T_s$, the surface temperature measured with the onboard infrared radiometer, for the nine bare fields labeled in Figure 1 are plotted in Figure 3. Five flights were made between September 20 and 29, the end of the experiment.

For the nine fields, the surface soil moisture decreased from September 20 to 29. The shape of the decrease varies from one field to another. The drying cycle can be divided into two stages. The first period is characterized by a decrease of the water content, the rate being different for each field, ranging from 0.04 $cm^3/cm^3$ per day for field 6 to 0.009 for field 3. The second stage, which does not begin at the same time for all parcels, is marked by little change in the radar signal, which can be interpreted as a level value in the water content decrease.

Adjacent fields have roughly the same behavior inasmuch as fields 1 and 2, fields 3, 7, and 8, and fields 4 and 6 exhibit similar drying cycles. The water content of field 5 is estimated lower on the first day than the water content of the other fields. This fact can be explained by the proximity of the small area of trees, which may, by their evaporative demand, act as a drain.

The surface temperature does not appear to be very different from one field to another. The general trend is that the driest fields have the highest temperature. This is certainly true for the last and driest days, September 26, 28, and 29. But the temperature differences never exceed 0.5° from the mean value.

## 4. INTERPRETATION

The main difference between the fields is that the radar signal (or equivalently, the moisture obtained using the regression line (1)) ceased to decrease at a point in time that depends on the field. Prior to September 23, fields 4 and 6 are the first to reach a plateau, followed by fields 1, 2, 3, 5, and 9 between September 23 and 26; in fields 7 and 8 the moisture decreases slowly until September 28 or 29. It is important to note that if the absolute value of the surface moisture were affected by a calibration error not exceeding the residual variance of 0.018 $cm^3/cm^3$ (Figure 3) due to instrumental problems (fading reduction, error on soil moisture ground truths) or to interactions between electromagnetic waves and surfaces (among them is roughness effect, which has been attenuated in the present experiment [*Ulaby and Batlivala*, 1976]), the relative variation for one field would certainly be significant.

Our approach is now to eliminate the evaporation flux heterogeneities and subsequently to quantify the time variation differences from one field to another in terms of water exchange between the surface layer seen by the radar and the underlying soil. The methodology is based on a two-layer model utilizing a diffusivity type of force-restore relationship used in models describing the interaction between soil and atmosphere [*Deardorff*, 1977; *Dickinson*, 1984]. Although this model is less realistic than the numerical solution of the Richards equation, it is as realistic as the reservoir algorithms used in watershed hydrological models to represent the unsaturated zone [*Holtan et al.*, 1975; *Girard*, 1974; *Ledoux*, 1980].

### 4.1. *Description of the Model*

After rainy days from September 16 to 19, the data plotted in Figure 3 show that the evolution of $w$ can be divided into two stages. The first is characterized by a decrease in water content, which is everywhere much larger than the measurement accuracy. The second stage is marked by a slow variation in time of the mean moisture in which the fluctuations are far smaller than the error bars. Such behavior can easily be modeled using the Richards equation. Previous studies [*Bernard et al.*, 1981; *Camillo and Schmugge*, 1984] have shown that the existence of two stages can be attributed to an increase of resistance to evaporation due to the near-surface layer dryness or the establishment of equilibrium between evaporation and capillary water pumping. In any case, the date and depth at which the level value begins depend heavily on the hydraulic properties of the surface and on the hydraulic state of the underlying soil. It is difficult to express the water budget of the first 10 cm of a real soil by the Richards equation resolution. This is due to the fact that water pressure head function $h$ and hydraulic conductivity $K$ must be known, together with the initial water content profile. If the Richards equation can be used to control the water budget of the soil from microwave remote sensing data [*Prévot et al.*, 1984], such a method cannot be used without any knowledge of the functions $h$ and $K$. This approach is not compatible with the aim of aerospace remote sensing, which is the estimation of regional surface properties. Hence the interpretation of the curves obtained from ERASME in terms of the water budget of the surface layer must be done using a simpler but still physically coherent model.

In this model the soil is represented as a two-layer system

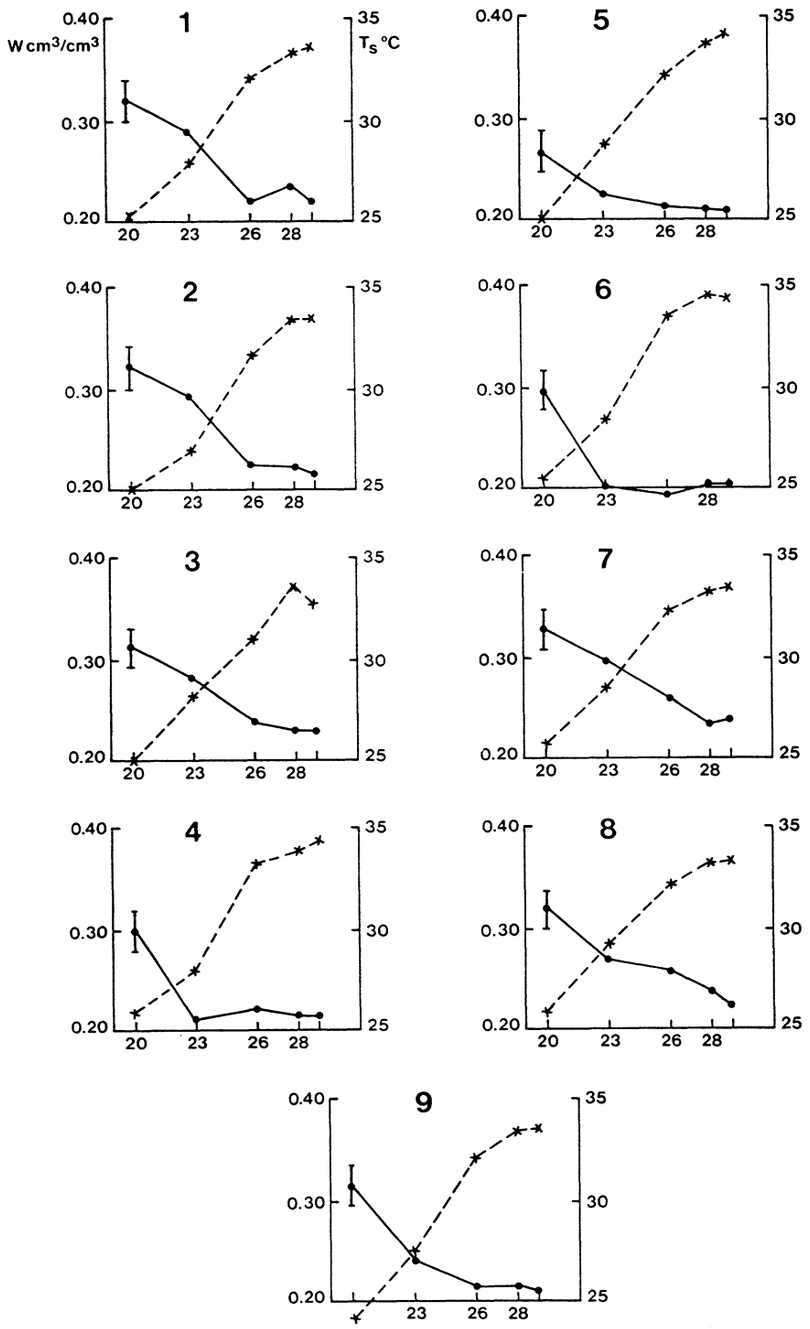


Fig. 3. The 0- to 10-cm layer water content ($w$) and the surface temperature ($T_s$) measured by ERASME remote sensing equipment during the 9-day period. Each figure corresponds to one of the fields labeled on the map in Figure 1. Heterogeneities of the soil water variations are clearly visible. The surface temperature does not exhibit the same features.

(Figure 4). The first layer, from the surface to $Z$, is a layer within which the mean moisture content $w$ obtained from ERASME (with the regression line (1)) provides a description of the hydraulic state ($Z$ may be equal to 10 cm). The second, beginning at $Z$, has a mean moisture content $V$. The variation of water content of the first layer expressed as water height ($Z\ \partial w/\partial t$) is equal to the difference between the incoming and outgoing fluxes. As no rain occurs during the 9-day period, the flux at the surface is evaporation $E$ (g/cm²). The flux through the boundary between the two layers is due to the capillary forces and to gravity. The gravity effect is, in general, negligible. Movement due to the capillary forces can be described as a diffusion process; it is proportional to the moisture gradient at the interface [*Philip and de Vries*, 1957]. The water budget equation for the surface layer can then be written

$$\frac{\partial w}{\partial t} = -\frac{E}{Z} + C(V - w) \qquad (2)$$

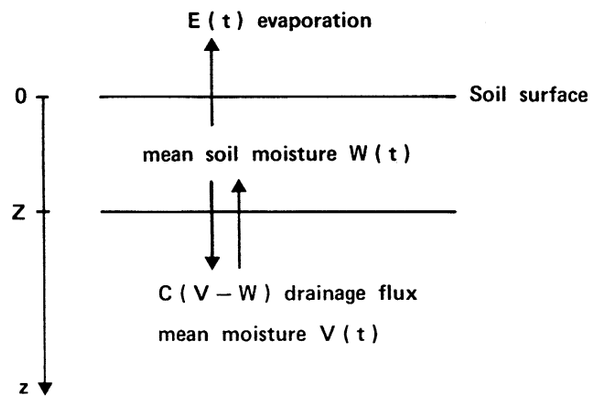


Fig. 4. Representation of the two-layer model used to follow the water budget of a bare soil surface layer.

$C$ represents pseudodiffusivity, and its unit is $T^{-1}$. It is a function of $Z$ and of the soil hydraulic state represented by $V$ and $w$. Although (2) is very approximate (in particular, it does not account for the moisture gradient in the layer below the soil surface if evaporation occurs), the main physical processes are represented, and it is sufficiently simple to quantitatively compare the fields' behavior. Moreover, it is perhaps the most complicated arrangement that can be constructed given the data that could be obtained from any space-borne measurement of surface soil moisture.

### 4.2. *Application to the September 1983 Experiment*

For each field, labeled $i$, one can write the expression (2)

$$w_i'(t) = -\frac{E_i(t)}{Z} + C_i(v_i, z)[V_i(t) - w_i(t)] \tag{3}$$

where $w_i'(t) = \partial w_i/\partial t$.

If the experiment duration is sufficiently short as to minimize drainage lost below about 1 m and if the evaporative demand is limited, then variation of the hydraulic state $V_i$ is small. Hence $V_i$ can be considered as constant; similarly, $C_i$ is considered as constant at first order (linear approximation of the Richards equation) during the period. If a field, labeled $r$, is taken as a reference, any quantity $Q_i$ can be written in the following form:

$$Q_i = Q_r + \Delta Q_i \tag{4}$$

Using (3) for fields $r$ and $i$, the quantities $\Delta Q_i$ are related by

$$\Delta w_i' = -\frac{1}{Z}\Delta E_i(t) + \Delta a_i - C_r \Delta w_i - \Delta C_i w_i \tag{5}$$

$$\Delta a_i = C_i \Delta V_i + V_r \Delta C_i$$

With the hypothesis of small variation of $V_i$, $\Delta a_i$ and $C_i = C_r + \Delta C_i$ do not depend on time and are, for the considered period of the year, an expression of field heterogeneities.

The scatterometer ERASME was in operation 5 days between September 20 and 29, yielding five sets of $w_i$ data (for fields $i$ = 1–9) (Figure 3). Taking one field as a reference, this leaves eight sets of $\Delta w_i$ values; it is then possible to obtain, by linear interpolation and finite difference, four sets of $(w_i, w_i')$ couples. Therefore $4 \times 8 = 32$ equations (5) can be written for the 25 unknowns $\Delta E_i(t)$, $\Delta a_i$, $C_r$, and $\Delta C_i$. It $\Delta E_i(t)$ is estimated for each day using other information, the 17 remaining unknowns can be found by ordinary least squares linear regression. It will be possible, using the measured water content of the first 60 cm of field 3 (see section 2.1), to verify that the variation of $V_i$ due to evaporation during the experiment is small.

TABLE 2. Daily Evaporation

| | September | | | |
|---|---|---|---|---|
| | 20 | 23 | 26 | 28 |
| Hour of Flight, LT | 1230 | 1115 | 1400 | 1200 |
| Field | | | | |
| 1 | 0.9 | 1.72 | 0.57 | 1.32 |
| 2 | 0.9 | 1.94 | 0.64 | 1.3 |
| 3 | 0.9 | 1.62 | 0.82 | 1.22 |
| 4 | 0.67 | 1.67 | 0.24 | 1.17 |
| 5 | 1.00 | 1.5 | 0.52 | 1.22 |
| 6 | 0.78 | 1.57 | 0.17 | 1.0 |
| 7 | 0.72 | 1.54 | 0.52 | 1.33 |
| 8 | 0.7 | 1.37 | 0.52 | 1.34 |
| 9 | 1.02 | 1.8 | 0.52 | 1.3 |

Daily evaporation is expressed in millimeters of water, *Seguin and Itier* [1983]: $E_d = R_{nd} + 0.25\,(T_s - T_a) + 0.95$.

It has been shown experimentally [*Jackson et al.*, 1977; *Seguin et al.*, 1982*a*, *b*] and theoretically [*Itier and Riou*, 1982; *Seguin and Itier*, 1983] that the evaporation above a natural ground surface can be statistically evaluated by a linear relationship between daily net radiation, daily evaporation, and the difference between maximum soil surface temperature $T_s$ and the air temperature $T_a$, 2 m above the surface; at the same time,

$$E_d = R_{nd} + B(T_s - T_a) + A \tag{6}$$

where $E_d$ is daily evaporation and $R_{nd}$ is daily net radiation, both expressed in millimeters of water.

*Seguin and Itier* [1983] show that for a bare soil, $B = 0.25$ mm $°C^{-1}$ and $A = 0.95$ mm. They have determined the accuracy of the estimation to be 20% on a 10-day basis. $R_{nd}$ is a function of surface albedo and temperature, but for same kind of surface and for relatively small variations of $T_s$, its variations are negligible compared with the term $B(T_s - T_a)$. Table 2 gives $E_{d_i}(t)$ for each field and each day calculated using the Seguin and Itier formula. Due to small heterogeneities on $T_s$ (see section 3.2 and Figure 3), the evaporation spatial variation appears to be small compared with the other terms (this will be verified later) and $\Delta E_i$ can be taken as zero for all times. Expression (5) then becomes

$$\Delta w_i' = \Delta a_i - C_r \Delta w_i - \Delta C_i w_i \tag{7}$$

Having eliminated the terms $\Delta E_i(t)$, the set of 32 equations is solved using field 3 as the reference field ($r = 3$). Results are listed in Table 3. The quality of the solutions, and therefore

TABLE 3. Pseudodiffusivity $C$ and Mean Water Content $V$ for Each Field Using the Simplified Water Budget Model

| Field | $\Delta a_i$ | $\Delta C_i$ | $C_i$, day$^{-1}$ | $V_i$, cm$^3$/cm$^3$ |
|---|---|---|---|---|
| 1 | −0.01 | −0.024 | 0.42 | 0.27 |
| 2 | −0.036 | −0.130 | 0.31 | 0.28 |
| 3 | 0.0 | 0.0 | 0.44 | 0.28 |
| 4 | 0.179 | 0.855 | 1.30 | 0.23 |
| 5 | 0.125 | 0.620 | 1.06 | 0.23 |
| 6 | 0.119 | 0.649 | 1.09 | 0.22 |
| 7 | 0.0 | −0.024 | 0.42 | 0.29 |
| 8 | 0.005 | 0.026 | 0.47 | 0.27 |
| 9 | 0.041 | 0.232 | 0.67 | 0.24 |

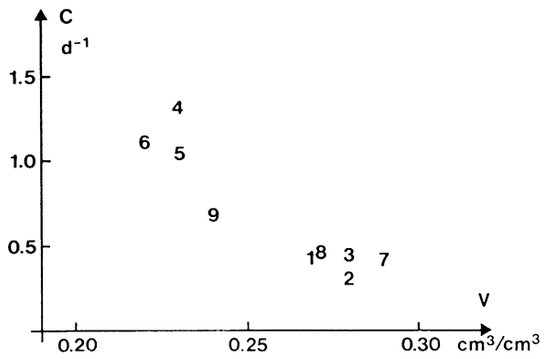


Fig. 5. Location of the fields in a pseudodiffusivity/mean water content diagram that may be used in soils classification.

the validity of the model, can be evaluated from the correlation coefficient between the measured and predicted differential slope $\Delta w_i'$. Its value of 0.76 with 14 degrees of freedom shows that the regression is significant. At this stage, the hypothesis of the negligible evaporation heterogeneities can be verified. Two values of $C$ are actually obtained (0.4 and 1.3). At the beginning of the period, the differential diffusion between the two groups of fields is then of the order of 0.05 $cm^3/cm^3$, which must be compared with the value of the differential evaporation, which is of the order of 0.003 $cm^3/cm^3$ in one day.

Using the water content of field 3 in the 0- to 60-cm top layer obtained on September 16 and adding rainfall, $V_3$ can be estimated as 0.28 $cm^3/cm^3$. It is this value that has been used to obtain $V_i$ ($i = 1, 9$) from $\Delta a_i$ and $C_i$. It is also possible to evaluate the cumulative evaporation over field 3 from September 20 to 29 using an integral form of (2):

$$-\int_{20}^{29} E(t)\,dt = Z(w_{29} - w_{20}) + ZC\int_{20}^{29} (v - w)\,dt \quad (8)$$

where $Z = 10$ cm.

The cumulative evaporation is found to be equal to 14 mm of water, which represents an 8% variation of $V_3$. Thus the hypothesis of $V_i$ invariance is confirmed. Furthermore, cumulative evaporation over field 3 calculated using Table 2 is found to be 12 mm of water, which is in good agreement with the evaluation based upon (8).

There are significant spatial heterogeneities in the pseudodiffusivity $C$ and in the mean water content $V$. For each field, notably during the first days, there is evaporation and drainage; the mean moisture content of the first layer ($w_i$) remains everywhere greater than the mean hydraulic state $V_i$. The drainage speed is variable, the pseudodiffusivity ranging from 0.3 (field 2) to 1.3 $day^{-1}$ (field 4). Finally, an equilibrium between evaporation and capillary pumping is reached, at which time the values of $w_i$ are smaller than $V_i$.

The methodology presented here characterizes each field by two parameters, $C$ and $V$. On a ($C$, $V$) diagram (Figure 5), one can note that, except for field 9, the fields are clustered in two regions. Fields belonging to the same region of the diagram are also in geographical proximity (Figure 1). This is true also for a classification using $C$ alone. Figure 5 does not represent an evaluation of a function $C(V)$; the hydraulic properties of the fields have no reason to be identical, and usually, the diffusivity is a growing function of $V$. The fact that the higher pseudodiffusivities are associated with the lower values of hydraulic state may be explained by the fact that a high value of $C$ implies a higher rate of drainage and ultimately a drier soil.

## 5. Conclusion

From a 9-day experiment, an airborne active microwave instrument has been shown to be capable of monitoring a drying cycle of a bare soil surface layer. Using the mapping capability of the airborne remote sensing, it has been shown that the technique can be used to estimate spatial drying heterogeneities. Spatial variations were interpreted as being due to different drainage properties between the surface layer and the underlying soil. A simple model, dealing with the water budget of the first 10 cm of a soil and accommodating only evaporation and capillary flow, has been used to define a pseudodiffusivity. This parameter is calculated for each field sampled remotely. The spatial heterogeneity of the drying cycles can then be evaluated using this pseudodiffusivity. For example, it can be used to classify soils; in this case the fields having similar pseudodiffusivities are adjacent. Accordingly, one can define homogeneous areas relative to the surface draining capability, expressed by the parameter $C_i$. In these measurements, $C_i$ ranged between 0.3 and 1.3 $day^{-1}$.

Although the proposed model is physically coherent, further analyses are needed. Using (8), the water flux at the interface of the two layers can be calculated. It will be necessary to verify this approach by comparing the actual amount of drained water and the calculated one. The pseudodiffusivity is a function of the soil hydraulic state. The stability of the field classification based on this parameter must be verified over a wide range of hydraulic states. Finally, the use of microwave remote sensing data proposed here may be useful in several domains, among them a quantitative description of soils for deriving parameters in atmospheric or watershed hydrologic models. Measuring drainage capability of the soil surface may also be directly applicable to problems in agricultural water management, such as irrigation and drainage or seed germination.

*Acknowledgments.* The authors would like to thank their colleagues at the Institut National de la Recherche Agronomique and Institut de Mécanique de Grenoble, who participated in the experiments, and the crew of the Centre National d'Etudes des Télécommunications helicopter. This research has been supported by the Centre National d'Etudes Spatiales, the Centre National de la Recherche Scientifique, and the Centre National d'Etudes des Télécommunications.

## References

Bernard, R., and D. Vidal-Madjar, ERASME: Diffusiomètre héliportable en bande C: Application à la mesure de l'humidité des sols, Proceedings of ERASEL/ESA Symposium on Remote Sensing Applications for Environmental Studies, *ESA SP 188*, pp. 59–64, Eur. Space Agency, Paris, France, 1983.

Bernard, R., M. Vauclin, and D. Vidal-Madjar, Possible use of active microwave remote sensing data for prediction of regional evaporation by numerical simulation of soil water movement in the unsaturated zone, *Water Resour. Res.*, *17*(6), 1603–1610, 1981.

Bernard, R., P. Martin, J. L. Thony, M. Vauclin, and D. Vidal-Madjar, C band radar for determining surface soil moisture, *Remote Sensing Environ.*, *12*, 189–200, 1982.

Bernard, R., O. Taconet, D. Vidal-Madjar, J. L. Thony, A. Chapoton, F. Wattrelot, and A. Lebrun, Comparison of three in situ surface soil moisture measurements and application to C band scatterometer calibration, *IEEE Trans. Geosci. Electron. Remote Sens.*, *GE-22*(4), 388–394, 1984.

Bradley, E. A., and F. T. Ulaby, Aircraft radar response to soil moisture, *Remote Sensing Environ.*, *11*, 419–438, 1981.

Camillo, P. J., and J. T. Schmugge, Correlating rainfall with remotely

sensed microwave radiation using physically based models, *IEEE Trans. Geosci. Electron. Remote Sens., GE-22*(4), 415–423, 1984.

Deardorff, J. W., A parameterization of ground surface moisture content for use in atmospheric prediction models, *J. Atmos. Meteorol., 16*, 1182–1185, 1977.

Dickinson, R. E., Modelling evapotranspiration for three-dimensional global climate models, in *Climate Processes and Climate Sensitivity, Geophys. Monogr. 29, Maurice Ewing Ser., vol. 5*, edited by J. E. Hansen and T. Takahashi, pp. 58–72, AGU, Washington, D. C., 1984.

Girard, G., Modèle global Orstom, Première application du modèle journalier à discrétisation spatiale sur le bassin versant de la crique Grégoire, en Guyanne, in *Atelier Hydrologique sur les Modèles Mathématiques*, ORSTOM, Paris, 1974.

Holtan, H. N., F. J. Stiltner, W. H. Henson, and N. C. Lopez, USDAHL-74, Revised model of watershed hydrology, *Tech. Bull. 1518*, Agric. Res. Serv., U.S. Dep. of Agric., Washington, D. C., 1975.

Itier, B., and Ch. Riou, Une nouvelle méthode de détermination de l'évapotranspiration réelle par thermographie I.R., *J. Rech. Atmos., 16*, 113–125, 1982.

Jackson, R. D., R. T. Reginato, and S.B. Idso, Wheat canopy temperature: A practical tool for evaluating water requirements, *Water Resour. Res., 13*, 651–656, 1977.

Jackson, T. J., A. Chang, and T. J. Schmugge, Aircraft active microwave measurements for estimating soil moisture, *Photogram. Eng. Remote Sensing, 47*, 801–805, 1981.

Ledoux, E., Modélisation intégrée des écoulements de surface et des écoulements souterrains sur un bassin hydrologique, Thèse de Docteur Ingénieur, Ecoles Nat. Supérieure des Mines de Paris et Univ. P. et M. Curie, Paris, 1980.

Mo, T., T. J. Schmugge, and T. J. Jackson, Calculations of radar backscattering coefficient of vegetation covered soils, *Remote Sensing Environ., 15*, 119–133, 1984.

Nielsen, D. R., J. W. Biggar, and K. T. Erh, Spatial variability of field measured soil water properties, *Hilgardia, 42*, 215–259, 1973.

Philip, J. R., Water movement in soil, in *Heat and Mass Transfer in the Biosphere*, edited by D. A. de Vries and N. H. Afgan, pp. 29–48, Scripta Book Company, New York, 1975.

Philip, J. R., and D. A. de Vries, Moisture movement in porous materials under temperature gradients, *Eos Trans. AGU, 38*, 222–232, 1957.

Prévot, L., R. Bernard, O. Taconet, and D. Vidal-Madjar, Evaporation from a bare soil evaluated from a soil water transfer model, using remotely sensed surface soil moisture data, *Water Resour. Res., 20*, 311–316, 1984.

Schmugge, T. J., Effect of soil texture on the microwave emission from soils, *IEEE Trans. Geosci. Electron., GE-18*, 353–361, 1980.

Seguin, B., and B. Itier, Using midday surface temperature to estimate daily evaporation from satellite thermal IR data, *J. Remote Sensing, 4*, 371–383, 1983.

Seguin, B., S. Baelz, J. M. Monget, and V. Petit, Utilisation de la thermographie infra rouge pour l'estimation de l'évaporation régionale, 1, Mise au point méthodologique sur le site de la Crau, *Agronomie, 2*(1), 7–16, 1982*a*.

Seguin, B., S. Bally, J. M. Monget, and V. Petit, Utilisation de la thermographie infra rouge pour l'estimation de l'évaporation regionale, 2, Résultats obtenus à partir des données de satellite, *Agronomie, 2*(2), 113–118, 1982*b*.

Ulaby, F. T., and P. P. Batlivala, Optimum radar parameters for mapping soil moisture, *IEEE Trans. Geosci. Electron., GE-14*(2), 81–93, 1976.

Ulaby, F. T., C. T. Allen, and A. K. Fung, Method for retrieving the true backscattering coefficient from measurements with a real antenna, *IEEE Trans. Geosci. Electron., GE-21*, 308–313, 1983.

Vauclin, M., S. R. Viera, R. Bernard, and J. T. Hatfield, Spatial variability of surface temperature along two transects of a bare soil, *Water Resour. Res., 18*, 1677–1686, 1983.

R. Bernard, J. V. Soares, and D. Vidal-Madjar, Centre National d'Etudes des Télécommunications, Centre National de la Recherche Scientifique/Centre de Recherche sur la Physique de l'Environment, 38/40 Rue du Général Leclerc, 92131 Issy-les-Moulineaux, France.

(Received April 22, 1985;
revised November 8, 1985;
accepted February 4, 1986.)